Steel and Composite Structures, *Vol. 31*, *No. 2* (*2019*) *125-131*
DOI: https://doi.org/10.12989/scs.2019.31.2.125

Mechanical behaviour of partially encased composite columns confined by CFRP under axial compression

Jiongfeng Liang [*1,2], Guangwu Zhang [2], Jianbao Wang [2] and Minghua Hu [2]

[1] *State Key Laboratory Breeding Base of Nuclear Resources and Environment*, *East China Institute of Technology*, *Nanchang*, *P.R. China*
[2] *Faculty of Civil & Architecture Engineering*, *East China Institute of Technology*, *Nanchang*, *P.R. China*

(*Received February 22, 2018, Revised September 21, 2018, Accepted April 2, 2019*)

Abstract. This paper presents the results of an experimental study to investigate the mechanical behavior of partially encased composite columns confined by CFRP under axial compression. The results show that the failure of the partially encased composite columns confined by CFRP occurred due to rupture of the CFRP followed by local buckling of the steel flanges. External wrapping of CFRP effectively delayed the local buckling of the steel flanges. The load carrying capacity of the column increased with the application of CFRP sheet. And the enhancement effect of the column was increased with the number of CFRP layer.

Keywords: column; CFRP; compression; enhancement; partially encased

1. Introduction

Composite columns have been widely used in high-rise buildings, highway bridges and offshore structures due to their load carrying capacity and energy dissipation characteristics. Conventional composite columns consist of steel and concrete and are typically classified as concrete-filled steel tubular (CFST) columns, concrete-encased steel (CES) columns and partially encased composite (PEC) columns. A PEC column is a type of composite column that generally consists of an H-shaped steel section with concrete cast between the flanges. One of the advantages for PEC column is that it requires formwork on only two sides of the column. Compared to reinforced concrete (RC) columns, PEC columns had an increased speed of erection because the steel shape was able to carry construction loads and also served as formwork for the concrete. In addition, PEC columns with smaller cross-section dimensions had similar axial resistance. Compared to bare steel columns, PEC columns had better resistance to fire and local buckling. And research has also been carried out on partially encased composite (PEC) columns (Dastfan and Driver 2018, Jamkhaneh and Kafi 2017, Pereira *et al*. 2017, Fellouh *et al*. 2017, Hanna and Gaawan 2016, Rocha *et al*. 2018). Pereira *et al*. (2016) evaluated the influence of replacing the conventional longitudinal and transverse steel bars by welded wire mesh on the structural behavior of partially encased composite columns under concentric loads. Begum *et al*. (2015) studied the overall column slenderness ratio, load eccentricity ratio, link spacing-to-depth ratio, flange plate slenderness ratio and concrete compressive strength on the behavior of thin-walled partially encased composite columns. Song *et al*. (2016) presented local and post-local buckling behavior of welded steel shapes in partially encased composite columns. Piquer and Hernández-Figueirido (2016) presented a comparison study between partially encased composite columns and I-shaped steel columns with and without protection. Mehdi and Robert (2016) found that modular steel plate shear wall with partially encased composite columns exhibited high initial stiffness, good displacement ductility and high energy dissipation capacity. Abdullah and Salih (2014) evaluated mechanical behaviour of partially encased composite beams and columns by finite element analysis method.

Fiber reinforced polymers (FRP) have been widely utilized in new construction as well as for the retrofit of existing structures (Fahmy and Wu 2018, Pham *et al*. 2018, Abbas *et al*. 2017, Nie *et al*. 2018, Chen *et al*. 2018a). A few studies have been made on the application of FRP in steel and concrete composite structures. Wang *et al*. (2014) studied the mechanical behavior of concrete-filled double skin steel tubular (CFDST) stub columns confined by fiber reinforced polymer (FRP). Park and Choi (2013) studied the structural behavior of CFRP (carbon fiber reinforced polymer) strengthened CFT (concrete-filled steel tubes) columns under axial loads. Chen *et al*. (2018b) experimentally investigated the axial compressive behavior of CFRP confined post heated square concrete-filled steel tube stub columns. It was found that the CFST stub columns wrapped with CFRP sheets shown a better mechanical behavior than those without CFRP sheets wrapping. Wang *et al*. (2018) reported an experimental and numerical analysis on eccentric compressive behavior of circular CFST stub columns partially-wrapped by CFRP strips. Wang *et al*. (2017) studied the static performance of axially compressed square concrete filled CFRP-steel

∗Corresponding author, Ph.D.,
E-mail: jiongfeng108@126.com

http://www.techno-press.org/?journal=scs&subpage=6
ISSN: 1229-9367 (Print), 1598-6233 (Online)

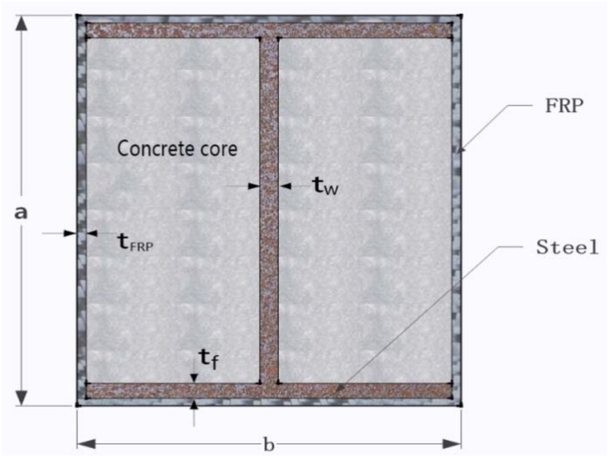

Fig. 1 Cross-section of partially encased composite columns confined by FRP

tubular (S-CF-CFRP-ST) columns. Shakir *et al*. (2016) studied the dynamic response of normal or recycled aggregate concrete-filled steel tube (NACFST and RACFST) columns subjected to lateral projectile impact and the effect of the Carbon Fibre Reinforced Polymer (CFRP) jacketing on the structural behavior of those columns.

In this study, a new composite column named partially encased composite columns confined by FRP has been proposed. This composite column consists of a steel column partially encased in concrete and wrapped with FRP sheet, as shown in Fig. 1. The additional FRP jacket is expected to enhance the axial behavior of the composite column by providing confinement to the concrete cores and preventing outward lateral buckling of the steel flanges. In order to understand the axial compressive behavior of partially encased composite columns confined by CFRP, an experimental program was carried out.

Table 1 Details of specimens in test

Specimen number	L (mm) (column length)	λ (slenderness ratio)	CFRP layers
C600-0	600	4.8	0
C600-1	600	4.8	1
C600-2	600	4.8	2
C600-3	600	4.8	3
C800-0	800	6.4	0
C800-1	800	6.4	1
C800-2	800	6.4	2
C800-3	800	6.4	3
C1000-0	1000	8.0	0
C1000-1	1000	8.0	1
C1000-2	1000	8.0	2
C1000-3	1000	8.0	3

2. Experimental programme

2.1 Test specimens

In this study, a total of twelve specimens, including 9 partially encased composite columns confined by CFRP, 3 unconfined partially encased composite columns were manufactured and tested under axial compression. All columns had a cross section of 125 mm × 125 mm. The hot rolled Q235 H steels were used in this test, which the nominal section sizes (D×B×tw×tf) were 125 mm × 125 mm × 6.5 mm × 9 mm, where D is the height of the H steel; B is the width of the H steel; tw is the web thickness of the H steel; tf is the flange thickness of the H steel. The parameters in the tests included: the numbers of CFRP layers (i.e., zero, one, two or three), slenderness ratio of the columns (i.e., 4.8, 6.4, or 8). Details of these specimens are given in Table 1.

2.2 Material properties

Normal strength concrete with a design compressive strength of 30 MPa at 28 days was used for casting the columns. Cubic compressive strength was determined by testing standard concrete cube (150 mm × 150 mm × 150 mm) according to GB50010-2010.

The average cubic compressive strength of concrete was 34.5 MPa.The nominal thickness and width of each layer of CFRP sheet were 0.167 mm and 100 mm, respectively. The ultimate tensile strength and elastic module of CFRP sheet was 3471 Mpa and 255 GPa. The mechanical properties of the H-steel used in this research are listed in Table 2.

2.3 Test setup and instrumentation

Fig. 2 shows the axial compression test setup. A microcomputer controlled electro-hydraulic servo testing machine YAW-3000 with 3000 kN was employed in the test. Each specimen was placed at the center of the machine for central axial compression loading. That was, all specimens were simply supported at the two ends, and the

Fig. 2 Test setup

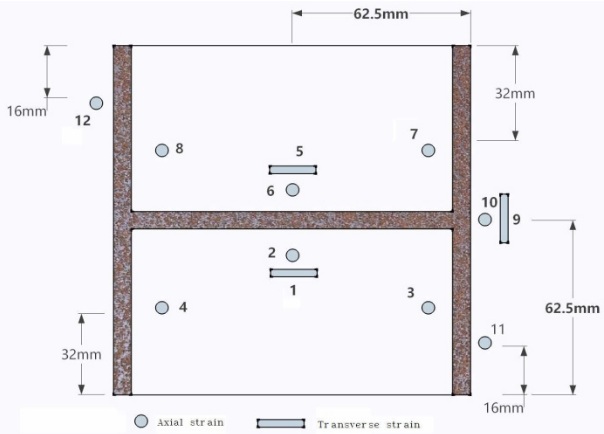

Fig. 3 Arrangements of strain gauges

Table 2 Properties of H-steel

H-steel	f_y (MPa)	f_u (MPa)	E_s (GPa)
Flange	348	482	203
Web	347	488	201

loading (or prescribed displacement) was exerted axially. he specimens were tested in a displacement controlled mode with a rate of 0.5 mm/min (Yoo *et al*. 2017) to observe detailedly failure procedures of specimens and local buckling.Two linear variable differential transducers (LVDTs) were set up inside the bottom end plate to monitor axial deformation. In addition, the strain gauges were attached to the H-steel surface and located at the midpoint of the specimen in the transverse direction and longitudinal direction to measure the transverse strain and the axial strain, respectively, as showed in Fig. 3. Data from the LVDTs and the strain gauges were collected by the DH3816N strain measurement system. The axial load was recorded automatically by the control system of the test machine. All data were recorded at every two seconds.

3. Results and discussion

3.1 Failure modes

All the partially encased composite columns confined by CFRP had some common failure phenomena under axial compression. In the initial stage, there were no obvious changes in the appearance of the specimens. With the increase of the load, the sound of resin cracking could be heard. As the load increased further, local buckling of specimens appeared near to the mid-height of the column. When the load reached about ninety percent of the ultimate load, the CFRP gradually ruptured and the lateral expansion of the specimens was obvious. It was indicated that lateral expansion of the specimens, which should be a lateral motion due to the buckling effect, caused the rupture of CFRP. Finally, the columns failed belong to the rupture of CFRP together with local buckling at the same location. Fig. 4 shows the failure modes of partially encased composite columns confined by CFRP.

Fig. 4 Failure modes of partially encased composite column confined by CFRP (C800-1)

Fig. 5 Failure modes of partially encased composite column (C600-0)

Fig. 5 shows the failure modes of partially encased composite columns not confined by CFRP after axial compression. It can be seen from Fig. 5 that the partially encased composite columns not confined by CFRP failure due to concrete crushing combining local buckling of the steel flanges. Compared to partially encased composite columns not confined by CFRP, the failure ductility of partially encased composite columns confined by CFRP could be further improved by utilizing angular fiber jackets.

3.2 Load versus strain relationships

Fig. 6 shows the typical load-strain curves of the specimens. It is shown that the load-strain curves consisted of three stages, namely elastic stage, elastic-plastic stage and plastic stage. The strain increased linearly with the increase of load within elastic stage. And the growth rate of the strain in the elastic-plastic stage and plastic stage was smaller than elastic stage for the specimens. The transverse strain and axial strain of the specimen with more number of CFRP layers increased slower than those specimens with less number of CFRP layers. Besides, through the analysis of strain development of unwrapped CFRP specimens, it showed that the strain growth increased quicker than those

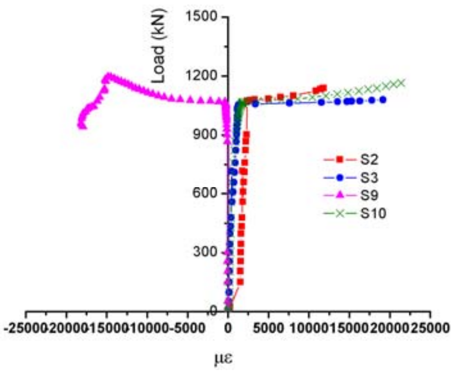

(a) C600-3

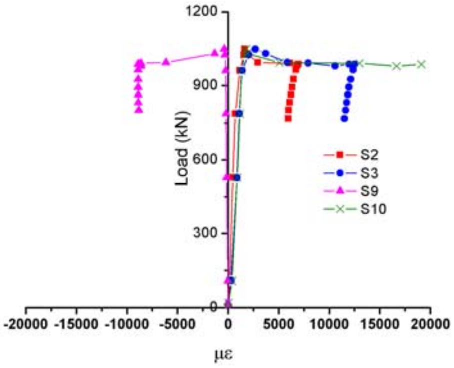

(b) C800-1

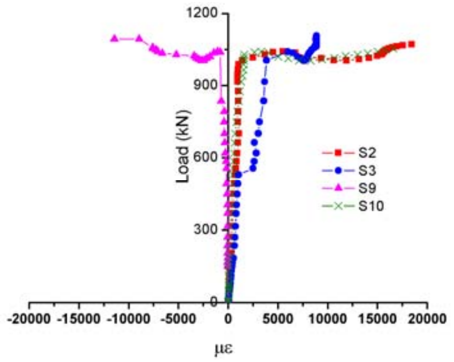

(c) C800-2

Fig. 6 Typical load-strain curves

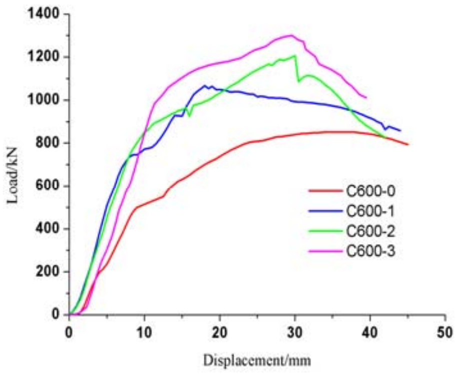

(a) C600-X

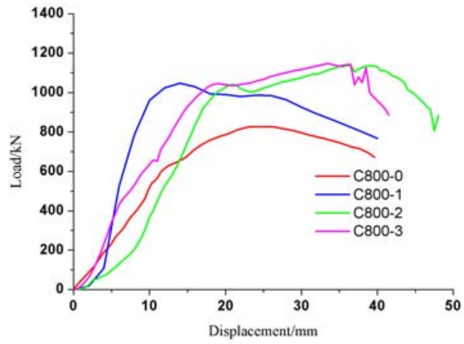

(b) C800-X

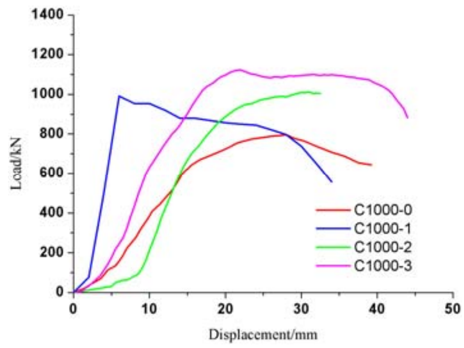

(c) C1000-X

Fig. 7 Load-displacement curves of specimens at different thickness of CFRP sheet

of wrapped with CFRP specimens. It was induced that CFRP confining lead to the enhancement of initial stiffness. This meant that the CFRP confining helped in reducing the local buckling of the steel plate.

3.3 Load versus displacement relationships

The axial load-axial displacement curves of all specimens are shown in Figs. 7 and 8. It can be found that the curves consist of three stages, namely the first initial stage, the elastic stage and the elastic-plastic stage. In the initial stage, axial load increased with the increase in axial displacement, and the slope of the curves was very gentle. As the load increased, the curve entered the elastic stage. In the elastic stage, the slope of curves in confined columns was larger than those of unconfined columns, and it showed that the confined columns had a higher stiffness modulus than those of columns. As the load continued to grow, the curve entered elastic-plastic stage. In this stage, the stiffness of the specimens decreased gradually. After the load achieved ultimate load, the axial load dropped suddenly and the curves bend sharply down due to the rupture of the CFRP.

Fig. 7 shows the effect of thickness of CFRP sheet on the load-displacement curve of specimens. From Figs. 7(a)~(c), the load-displacement curves of confined specimens had almost the same shape. The higher the thickness of the CFRP was, the greater the ultimate axial load of the confined specimens was. Besides that, the higher the thickness of CFRP was, the larger elastic-plastic deformation of confined specimens was. Fig.8 shows the effect of the slenderness ratio of CFRP sheet on the load-displacement curve of specimens. It can be seen that the shape of the load-displacement curves didn't change with the variation of the slenderness ratio if the slenderness ratio

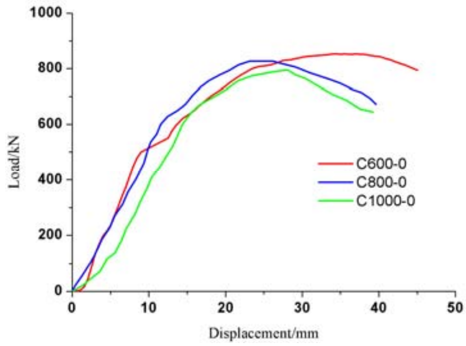

(a) CX-0

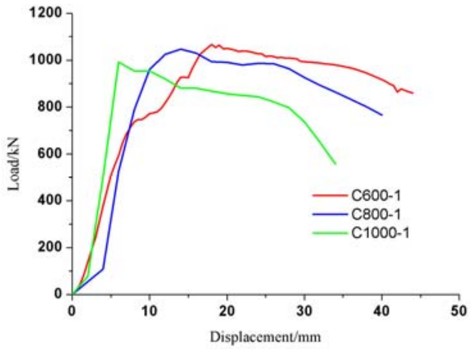

(b) CX-1

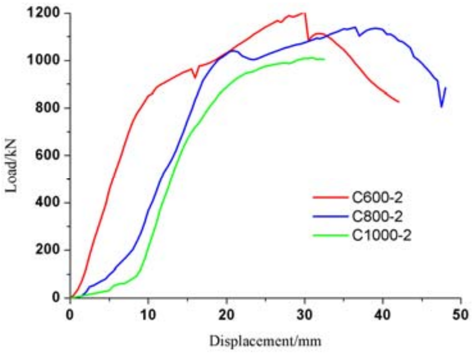

(c) CX-2

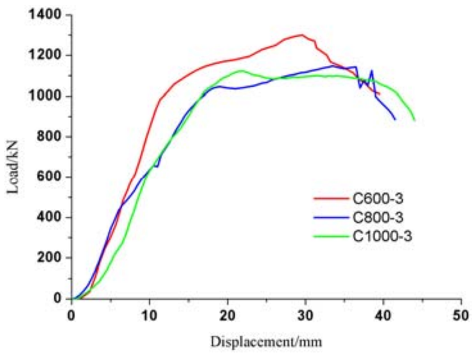

(d) CX-3

Fig. 8 Load-displacement curves of specimens at different slenderness ratio

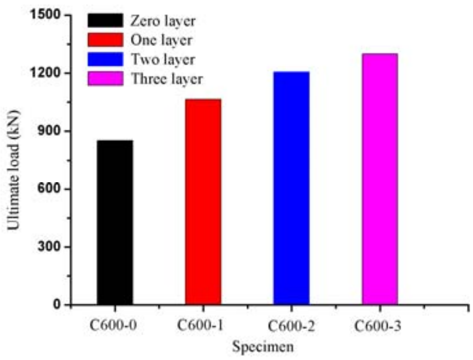

(a) Ultimate load for columns C600-comparison

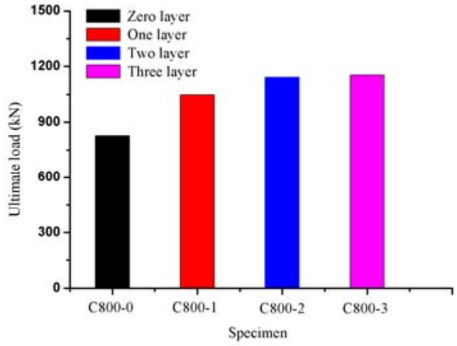

(b) Ultimate load for columns C800-comparison

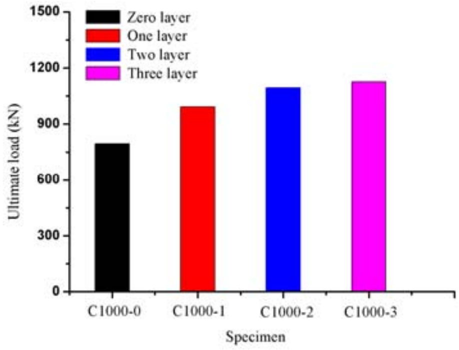

(c) Ultimate load for columns C1000-comparison

Fig. 9 Ultimate load versus thickness of CFRP sheet

was in the range from 4.8 to 8. The load-displacement curve of specimens with the thicker CFRP sheet had a longer elastic-plastic stage.

3.4 Axial load carrying capacity

Fig. 9 shows the ultimate load versus thickness of CFRP sheet. It can be seen that the ultimate load of specimens increased with the increasing thickness of CFRP sheet (i.e., the number of CFRP sheet layers).The specimens confined with CFRP such as C600-1,C600-2 and C600-3 had 25.2%, 41.5% and 52.5% more load carrying capacity than that of the control unconfined column C600-0,respectively,as showed in Fig. 9(a). When compared to column C800-0, columns C800-1, C800-2 and C800-3 increased their axial load carrying capacity by 26.7%, 37.9% and 39.3%, respectively. When compared to column C1000-0, columns C1000-1, C1000-2 and C1000-3 increased their axial load carrying capacity by 24.9%, 37.6% and 41.8%, respectively. Therefore, it had proved that the CFRP sheets and partially encased composite columns had the good bonding action and external bonding of CFRP sheets could be able to

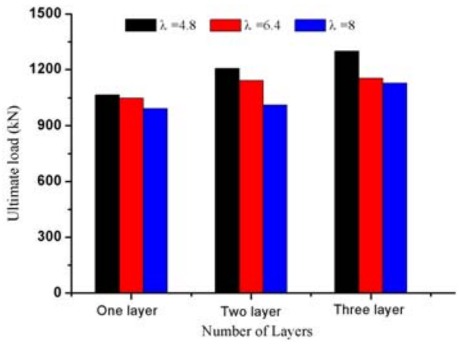

Fig. 10 Ultimate load versus slenderness ratio

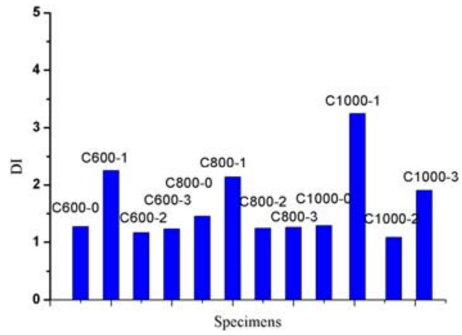

Fig. 11 Ductility index for all specimens

provide necessary confining pressure to the column were confined.

Fig. 10 shows the ultimate load versus slenderness ratio. It can be seen that the ultimate load of specimens decreased with the increasing slenderness ratio. For one-layer CFRP confined specimens, the axial load carrying capacity of specimen C800-1 with slenderness ratio λ = 6.4 was 1.8% less than that of specimen C600-1 with slenderness ratio λ = 4.8; the axial load carrying capacity of specimen C1000-1 with slenderness ratio λ = 8 was 7.2% less than that of specimen C600-1 with slenderness ratio λ = 4.8. For two-layer CFRP confined specimens, the axial load carrying capacity of specimen C800-2 with slenderness ratio λ = 6.4 was 5.3% less than that of specimen C600-2 with slenderness ratio λ = 4.8; the axial load carrying capacity of specimen C1000-2 with slenderness ratio λ = 8 was 9.3% less than that of specimen C600-2 with slenderness ratio λ = 4.8. For three-layer CFRP confined specimens, the axial load carrying capacity of specimen C800-3 with slenderness ratio λ = 6.4 was 11.3% less than that of specimen C600-3 with slenderness ratio λ = 4.8; the axial load carrying capacity of specimen C1000-3 with slenderness ratio λ = 8 was 13.2% less than that of specimen C600-2 with slenderness ratio λ = 4.8. It indicated that the slenderness ratio had some impact on the axial load carrying capacity of the confined specimens.

3.5 Ductility index

In order to quantify the ductility of columns, ductility index (DI) has been used in and defined as

$$DI = \frac{\delta(0.85N_u)}{\delta(N_u)} \quad (1)$$

Where $\delta(0.85N_u)$ is the displacement corresponding to 85% of the maximum load (in the descending branch of the load-displacement curve), $\delta(N_u)$ is the displacement corresponding to the maximum load, N_u is the maximum load.

Fig. 11 shows the ductility index for all specimens. It can be seen that the ductility index of specimens increased firstly and then decreased with the increasing thickness of CFRP sheet. The ductility index of C600-1, C600-2 and C600-3 was 177%, 91.8%, 96.9% of that to C600-0, respectively. The ductility index of C800-1, C800-2 and C800-3 was 147%, 85.3%, 86.7% of that to C800-0, respectively. The ductility index of C1000-1, C1000-2 and C1000-3 was 252%, 83.9%, 94.7% of that to C1000-0, respectively. And the average ductility index of the confined columns was about 1.3. The ductility index of the confined columns of two-layer CFRP or three-layer CFRP was similar to that of the unconfined columns; the ductility index of the confined columns of one-layer CFRP was higher than that of the unconfined columns. It indicated that partially encased composite columns confined by CFRP had good ductility.

4. Conclusions

Based on the experimental results, the following conclusions can be drawn:

- Failure of partially encased composite columns confined by CFRP occurred due to the rupture of the CFRP followed by local buckling of the steel flanges. External wrapping of CFRP effectively delayed the local buckling of the steel flanges.
- The ultimate load-bearing capacity of partially encased composite columns confined by CFRP increased with the increase of the number of CFRP layers. However, the increasing slenderness ratio decreased the load-bearing capacity of partially encased composite columns confined by CFRP.
- The ductility of partially encased composite columns confined by CFRP increased firstly and then decreased with the increasing number of CFRP layers.
- It had some enhancement in the strength, elastic axial stiffness and ultimate displacement of partially encased composite columns after confining. Confinement was enhanced by increasing the number of CFRP layers.

Based on the research results reported in this paper, it seemed that the number of CFRP layer, slenderness ratio had some influence on the load carrying capacity and ductility of partially encased composite columns confined by CFRP. Generally, the load bearing capacity of partially encased composite columns confined by CFRP will increase with the increasing material grades.To carry out compression behavior of partially encased composite columns confined by CFRP, further research was need to study on the influence of the material grades.

Acknowledgments

This work was supported by the Chinese National Natural Science Foundation (No. 51868001), the Natural Science Foundation of Jiangxi Province for Distinguished Young Scholars (No.20162BCB23051), the Natural Science Foundation of Jiangxi Province (No. 20171BAB206053), and the Open Project Program of Jiangxi Engineering Research Center of Process and Equipment for New Energy, East China Institute of Technology (No. JXNE-2014-08), which are gratefully acknowledged.

References

Abbas, T., Tim, I., Antony, D., Mark, E. and Pedro, S. (2017), "Prediction of Capacity for Moment Redistribution in FRP-Strengthened Continuous RC T-Beams", *J. Compos. Constr.*, **21**(1), 1-13

Abdullah, J.A. and Salih, O.A. (2014), "Behavior and design of partially-encased composite beam-columns", *Tikrit J. Eng. Sci.*, **20**(3), 24-36

Begum, M., Driver, R.G. and Elwi, A.E. (2015), "Parametric study on eccentrically-loaded partially encased composite columns under major axis bending", *Steel Compos. Struct., Int. J.*, **19**(5), 1299-1319

Chen, W.S., Pham, T.M., Sichembe, H., Chen, L. and Hao, H. (2018a), "Experimental study of flexural behaviour of RC beams strengthened by longitudinal and U-shaped basalt FRP sheet", *Compos. Part B-Eng.*, **134**, 114-126

Chen, Y., Wang, K., He, K., Wei, J.G. and Wan, J. (2018b), "Compressive behavior of CFRP-confined post heated square CFST stub columns", *Thin-Wall. Struct.*, **127**, 434-445

Dastfan, M. and Driver, R. (2018), "Test of a steel plate shear wall with partially encased composite columns and RBS frame connections", *J. Struct. Eng.*, **144**(2), 04017187

Fahmy, M.F.M. and Wu, Z. (2018), "Restoration of pre-damaged RC bridge columns using basalt FRP composites", *Earthq. Struct., Int. J.*, **14**(5), 379-388

Fellouh, A., Benlakehal, N., Piloto, P., Ramos, A. and Mesquita, L. (2017), "Load carrying capacity of partially encased columns for different fire ratings", *Fire Res.*, **1**, 380-390

GB50010-2010 (2010), National Standard of the People's Republic of China; Code for design of concrete structures, Chinese Architecture and Building Press, Beijing, China. (Only available in Chinese)

Hanna, E.M. and Gaawan, S.M. (2016), "Experimental testing of partially encased composite beam columns", *Int. J. Eng. Res. Appl.*, **6**(1), 64-71

Jamkhaneh, M.E. and Kafi, M.A. (2017), "Experimental and numerical investigation of octagonal partially encased composite columns subject to axial and torsion moment loading", *Civil Eng. J.*, **3**(10), 939-955.

Mehdi, D. and Robert, Q.D. (2016), "Large-scale test of a modular steel plate shear wall with partially encased composite columns", *J. Struct. Eng.*, **142**(2), 1-9

Nie, X.F., Zhang, S.S., Teng, J.G. and Chen, G.M. (2018), "Experimental study on RC T-section beams with an FRP-strengthened web opening", *Compos. Struct.*, **1**, 273-285

Pereira, M.F., De Nardin, S. and El Debs, A.L.H.C. (2016), "Structural behavior of partially encased composite columns under axial loads", *Steel Compos. Struct., Int. J.*, **20**(6), 1305-1322.

Pereira, M.F., Beck, A.T. and El Debs, A.L.H.C. (2017), "Reliability of partially encased steel-concrete composite columns under eccentric loading", *Rev.ibracon Estrut.mater*, **10**(2), 298-316.

Piquer, A. and Hernández-Figueirido, D. (2016), "Protected steel columns vs partially encased columns: Fire resistance and economic considerations", *J. Constr. Steel Res.*, **124**, 47-56.

Park, J.W. and Choi, S.M. (2013), "Structural behavior of CFRP strengthened concrete-filled steel tubes columns under axial compression loads", *Steel Compos. Struct., Int. J.*, **14**(5), 453-472.

Pham, T.M., Zhang, X., Elchalakani, M., Karrech, A., Hao, H. and Ryan, A. (2018), "Dynamic response of rubberized concrete columns with and without FRP confinement subjected to lateral impact", *Constr. Build. Mater.*, **186**, 207-218

Rocha, F.M., Rodrigues, J.P.C. and Neto, J.M. (2018), "Fire behavior of steel and partially encased composite columns embedded on walls", *J. Construct. Steel Res.*, **149**, 105-118.

Shakir, A.S., Guan, Z.W. and Jones, S.W. (2016), "Lateral impact response of the concrete filled steel tube columns with and without CFRP strengthening", *Eng.Struct.*, **116**, 148-162

Song, Y.C., Wang, R.P. and Li, J. (2016), "Local and post-local buckling behavior of welded steel shapes in partially encased composite columns", *Thin-Wall. Struct.*, **108**, 93-108

Wang, J., Liu, W.Q., Zhou, D., Zhu, L. and Fang, H. (2014), "Mechanical behaviour of concrete filled double skin steel tubular stub COLUMNS confined by FRP under axial compression", *Steel Compos. Struct., Int. J.*, **17**(4), 431-452.

Wang, Q.L., Qu, S.E., Shao, Y.B. and Feng, L.M. (2016), "Static behavior of axially compressed circular concrete filled CFRP-steel tubular (C-CF-CFRP-ST) columns with moderate slenderness ratio", *Adv. Steel Constr.*, **12**(3), 263-295.

Wang, Q.L., Zhao, Z., Shao, Y.B. and Li, Q.L. (2017), "Static behavior of axially compressed square concrete filled CFRP-steel tubular (S-CF-CFRP-ST) columns with moderate slenderness", *Thin-Wall. Struct.*, **110**, 106-122

Wang, J.F., Shen, Q.H., Wang, F.Q. and Wang, W. (2018), "Experimental and analytical studies on CFRP strengthened circular thin-walled CFST stub columns under eccentric compression", *Thin-Wall. Struct.*, **127**, 102-119

Yoo, S.W., Choi, Y.C. and Choi, W. (2017), "Compression behavior of confined columns with high-volume fly ash concrete", *Adv. Mater. Sci. Eng.*, 1-11.

CC